The Atmospheric Hydrologic Cycle over the Arctic Basin from Reanalyses. Part I: Comparison with Observations and Previous Studies*

RICHARD I. CULLATHER+ AND DAVID H. BROMWICH#

Polar Meteorology Group, Byrd Polar Research Center, The Ohio State University, Columbus, Ohio

MARK C. SERREZE

Cooperative Institute for Research in Environmental Sciences, Division of Cryospheric and Polar Processes, University of Colorado, Boulder, Colorado

(Manuscript received 10 July 1998, in final form 14 May 1999)

ABSTRACT

The atmospheric moisture budget is evaluated for the region 70°N to the North Pole using reanalysis datasets of the European Centre for Medium-Range Weather Forecasts (ECMWF; ERA: ECMWF Re-Analysis) and the collaborative effort of the National Centers for Environmental Prediction (NCEP) and the National Center for Atmospheric Research (NCAR). For the forecast fields of the reanalyses, the ERA annually averaged $P - E$ (precipitation minus evaporation/sublimation) field reproduces the major features of the basin perimeter as they are known, while the NCEP–NCAR reanalysis forecast fields contain a spurious wave pattern in both P and E. Comparisons between gauge data from Soviet drift camp stations and forecast P values of the reanalyses show reasonable agreement given the difficulties (i.e., gauge accuracy, translating location). When averaged for 70°–90°N, the ERA and NCEP–NCAR forecast $P - E$ are similar in the annual cycle. Average reanalysis forecast values of E for the north polar cap are found to be 40% or more too large based on comparisons using surface latent heat flux climatologies.

Differences between a synthesized average moisture flux across 70°N from rawinsonde data of the Historical Arctic Rawinsonde Archive (HARA) and the reanalysis data occur in the presence of rawinsonde network problems. It is concluded that critical deficiencies exist in the rawinsonde depiction of the summertime meridional moisture transport. However, it remains to be seen whether the rawinsonde estimate can be rectified with a different method. For 70°–90°N, annual moisture convergence ($P - E$) values from the ERA and NCEP–NCAR are very similar; for both reanalyses, annual $P - E$ values obtained from forecast fields are much lower than those obtained from moisture flux convergence by about 60%, indicating severe nonclosure of the atmospheric moisture budget. The nonclosure primarily results from anomalously large forecast E values. In comparison with other studies, reanalyses moisture convergence values are much more reasonable. A synthesis of the reanalysis moisture convergence values and more recent studies yields a value of 18.9 ± 2.3 cm yr^{-1} for the north polar cap.

1. Introduction

A quantitative depiction of the atmospheric hydrologic cycle over the Arctic basin has significant relevance to a variety of weather- and climate-related investigations. Reliable water vapor distributions are necessary for the accurate retrieval of surface parameters over the ice pack from satellites (e.g., Rossow et al. 1989; Key and Haefliger 1992) and for the validation of general circulation models (Randall et al. 1998). Moreover, precipitation over the Arctic basin is a primary input to the hydrologic budget. The variability in this supply of freshwater has the potential for affecting the stability of the Arctic halocline, with broader implications for oceanic circulation at lower latitudes. North Atlantic conditions are intimately related to the Arctic via ice and freshwater discharges through the Fram Strait (Mysak et al. 1990). Paleoclimate and oceanographic research over the last few decades has suggested that the stability of the North Atlantic thermohaline circulation has a significant impact on the climate system (Broecker 1997). The paleoclimate record and its implication of the North Atlantic as a center for

* Byrd Polar Research Center Contribution Number 1130.

+ Current affiliation: Department of Aerospace Engineering Sciences, University of Colorado, Boulder, Colorado.

Additional affiliation: Atmospheric Sciences Program, Department of Geography, The Ohio State University, Columbus, Ohio.

Corresponding author address: David H. Bromwich, Polar Meteorology Group, Byrd Polar Research Center, The Ohio State University, 1090 Carmack Road, Columbus, OH 43210-1002.
E-mail: bromwich@polarmet1.mps.ohio-state.edu

climate change underscore the importance of understanding the freshwater budget and its variability for the contemporary Arctic.

In the Arctic, the presence of a floating ice field creates difficult conditions for obtaining reliable precipitation depictions. Observational estimates of precipitation data are also hindered by the difficulty of obtaining accurate estimates of solid precipitation rates. Gauge-based measurements of precipitation rates are subject to biases imposed by wind turbulence over the gauge orifice, and because of the introduction of blowing snow from snow fields surrounding the measurement sites (Woo et al. 1983). Although efforts have been made to computationally address wind-induced biases, data postprocessing cannot address the meager number of long-term observational points in the historical record for polar regions. This presents a severe limitation to synthesizing a useful spatial depiction of precipitation (Bromwich et al. 1998a). These limitations have led to the exploration of atmospheric methods including reanalyses. Reanalyses are numerical depictions of the atmosphere that incorporate all available observations, including satellite data, using a ''frozen'' data assimilation system.

In this study, the atmospheric moisture budget for the Arctic basin and surrounding land areas north of 70°N is derived from reanalysis products of the European Centre for Medium-Range Weather Forecasts (ECMWF) and the collaborative effort of the National Centers for Environmental Prediction (NCEP) and the National Center for Atmospheric Research (NCAR). Rawinsonde, in situ gauge measurements, and observational estimates from previous studies are used for quantitative evaluation of the reanalysis data. The paper is organized in a fashion similar to previous global studies (e.g., Trenberth and Guillemot 1996b, 1998; Rasmusson and Mo 1996) by separately examining 1) the forecast precipitation (P) and evaporation/sublimation (E) fields, and 2) $P - E$ computed from analyzed wind, moisture, and surface pressure fields. The closure between the forecast variables and computed $P - E$ is then evaluated. By primarily focusing on the closure and discrepancies with previous observation, the veracity of the reanalysis datasets in high northern latitudes may be readily assessed. Some significant issues to be addressed are as follows.

- How well do the two reanalysis datasets agree with each other?
- How does $P - E$ computed from analyzed variables compare to the forecast fields?
- Are the reanalyses in agreement with previous observations? Are the causes of discrepancies apparent?

An important aspect of the third question is the comparison with results presented by Serreze et al. (1995a,b) using the Historical Arctic Rawinsonde Archive (HARA) of the National Snow and Ice Data Center (Serreze et al. 1992). The HARA record is an extensive dataset of available soundings north of 65°N. For reference, Fig. 1 shows the rawinsonde network distribution used by Serreze et al. (1995a,b) for computing moisture transports across 70°N, along with significant geographical features. Aside from various long-term climate atlases and satellite-derived precipitable water estimates, the rawinsonde network is the only source of observational data for the atmospheric hydrologic cycle over the north polar cap. Thus, it is necessary to identify and understand any disagreements with the rawinsonde-based estimates in order to have confidence in the reanalysis data.

2. Datasets and calculations

The concept of reanalysis has been described by Trenberth (1995) and Kalnay et al. (1996). Reanalyses represent an effort to remove the spurious trends found in archived operational analyses that are associated with evolving data assimilation techniques. The remaining temporal variability is then either real or the result of changes to the observational network. The ECMWF Re-Analysis (ERA) is described by Gibson et al. (1997). The ERA is produced four times daily using a spectral numerical weather prediction (NWP) model at T106 horizontal resolution with 31 hybrid levels in the vertical. The NCEP–NCAR reanalysis is also produced four times daily, at T62 horizontal resolution and 28 σ levels in the vertical. For this study, the ERA basic dataset and the NCEP–NCAR reanalyses were obtained from NCAR at 2.5° $\times$ 2.5° resolution at near-surface and standard pressure levels for the years 1979–93. Although this limits the resolution obtainable for the moisture flux convergence field, there are practical considerations associated with using reanalysis data. In an uncompressed, binary form, the size of the ERA 2.5° $\times$ 2.5°, standard pressure level data, and related fields is approximately 165 gigabytes.

As part of both reanalysis datasets, a series of short-term forecasts has been performed using each analysis center's NWP model, which has been initialized using reanalysis fields. This provides supplementary fields, including P and E, that are not directly observed or analyzed. These fields are more dependent on the physics of the NWP model utilized, however.

The computations described in this section are similar to those employed in Cullather et al. (1998); however, the software package of Adams and Swarztrauber (1997) is used to compute the atmospheric moisture convergence fields at T21 resolution. This eliminates the need for ad hoc finite difference schemes on the surface of the sphere. The surface moisture balance $P - E$ may be obtained by directly computing the atmospheric moisture budget from the analyzed variables. This is done using

$$P - E = -\frac{\partial W}{\partial t} - \nabla \cdot \mathbf{Q}, \qquad (1)$$

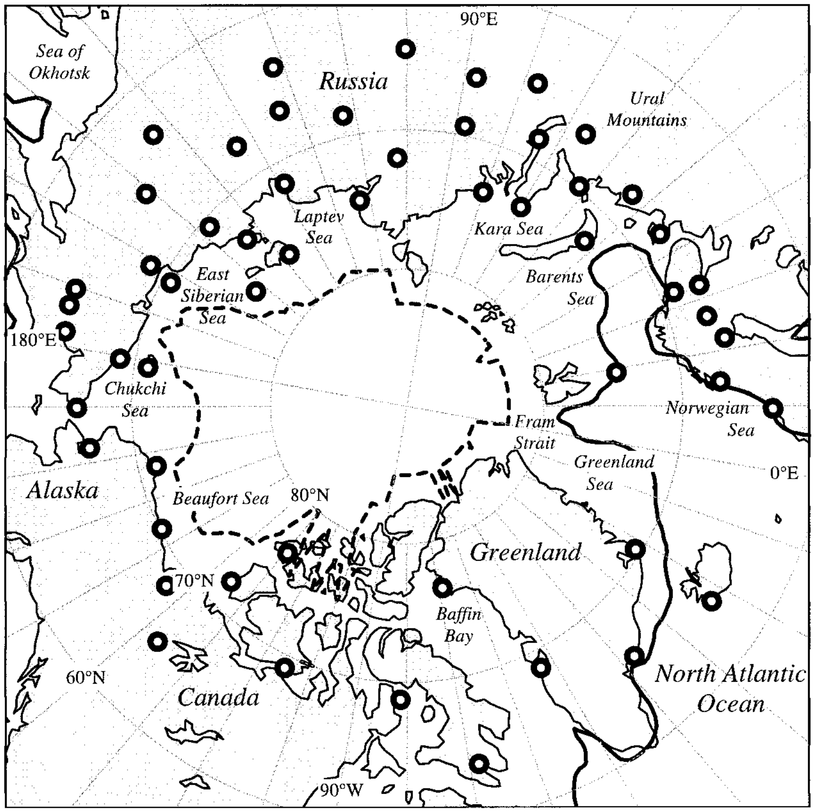

FIG. 1. Map of the Arctic basin. Solid and dashed lines indicate the average Jan and Jul extent of sea ice, as defined by the $-1.8°C$ surface temperature contour from the ERA. Rawinsonde stations used for computing the meridional atmospheric moisture transport across 70°N after Serreze et al. (1995a) are shown as open circles.

where W is precipitable water and $\mathbf{Q}$ is the atmospheric moisture transport, defined as

$$\mathbf{Q} = \frac{1}{g}\int_{P_{\mathrm{top}}}^{P_{\mathrm{sfc}}} q\mathbf{V}\, dp, \tag{2}$$

where g is the gravity constant, P_{sfc} is surface pressure, q is specific humidity, and $\mathbf{V}$ is the horizontal wind vector. The variable P_{top} is the highest level of the atmosphere, which is not zero in the analyses. For annual timescales, the first right-hand side term, referred to as the storage term, is considered negligible. Equation (1) may be computed at each point of a dataset to produce a field of $P - E$. In addition to the residual term obtained from the moisture budget, the flux itself is of interest because it contains information on the atmospheric circulation patterns that result in the distribution of $P - E$. The dominant features of these transport patterns have been referred to as atmospheric ''rivers'' (Newell and Zhu 1994; Trenberth and Guillemot 1996a).

When the forecast P and E fields are commensurate with the right-hand side of Eq. (1) computed from analysis values, the dataset is said to be in ''hydrologic balance.'' It is important to recognize the temporal differences between the two methods, however. The forecast fields are accumulated over some period of each forecast, while the atmospheric moisture budget is computed for a specified instant in time. The ERA forecast fields contained in the NCAR archive are obtained from the 12–24-h period of each forecast, while the NCEP–NCAR reanalysis utilizes the 0–6-h forecast. Thus for the ERA forecast fields, an estimate of $P - E$ for one day is determined from two 12–24-h forecasts. For NCEP–NCAR reanalyses, a one-day estimate of forecast $P - E$ is determined from four 0–6-h forecasts. For both datasets, $P - E$ computed via the atmospheric moisture budget is discretely sampled four times daily. To mitigate these temporal sampling effects, one typically averages the fields in space and time in order to evaluate the hydrologic balance of a dataset. Although it may not be sufficient for particular regions associated with unique phenomena, it is typically assumed that four times daily is sufficient to capture the major hydrologic features on climatic timescales such that Eq. (1) is expected to be satisfied (Trenberth and Guillemot 1996b, 1998). Hereafter, the expression ''computed $P - E$'' is used to refer to fields computed from analyzed wind, moisture, and surface pressure fields using Eq. (1), while ''forecast $P - E$'' refers to the reanalysis forecast variables.

Reanalysis data represent months or even years of computer processing time, and oversights would appear to be inevitable. For the NCEP–NCAR reanalysis in high northern latitudes, the relevant difficulties that have been identified are that the analyses were not produced using interannually varying snow cover for the period 1974–94 (E. Kalnay 1997, personal communication) and that the NWP model's horizontal diffusion parameterization is oversimplified. An additional comment on this latter point is given below. Difficulties in the production of the ERA are discussed by Kållberg (1997) and include a surface temperature cold bias in northern boreal forests during winter and springtime. The latent heat of freezing in ERA convection was also found to be erroneously set to zero. Globally, several studies have evaluated the atmospheric hydrologic cycle from reanalysis data (Stendel and Arpe 1997; Trenberth and Guillemot 1996b, 1998). These studies indicate differences with assembled global climatologies as well as demonstrate hydrologic imbalance in reanalysis data. The studies highlight the challenges of producing realistic global depictions of atmospheric moisture variables.

Several recent studies have investigated the performance of the reanalyses forecast P and E fields in polar regions. In particular, Serreze and Hurst (2000) have comprehensively examined the NCEP–NCAR and ERA forecast P in comparison to an improved gauge-based climatology. Both reanalyses were found to underestimate annual values over the Atlantic side of the Arctic. The most significant problem found was a tendency to produce too much convective precipitation over land areas in the NCEP–NCAR forecasts. Serreze and Maslanik (1997) have also examined the NCEP–NCAR forecast precipitation fields over the Arctic for the period 1986–93. For the NCEP–NCAR forecast fields, there is the provocative high-latitude spurious wave pattern that results from an overly simplified NWP model diffusion parameterization on constant pressure surfaces (W. Ebisuzaki 1996, personal communication). Serreze and Maslanik (1997) compensated for this by applying a Cressman filter to smooth the fields. The resulting fields were found to have a reasonable spatial distribution in comparison to available climatologies, with significant differences in seasonality over the central Arctic basin. For the forecast fields, the discussion presented below is constrained to an overview of the previously reported results and an emphasis on results not presented elsewhere. An overview of NCEP–NCAR forecast spatial patterns is useful for comparison with the ERA. Additionally, the computed $P - E$ fields presented here provide additional context for evaluating the forecast fields.

3. Forecast P, E, and $P - E$

For the central Arctic basin, the long-term average fields of forecast $P - E$ have been computed from the two reanalysis datasets for the period 1979–93 and have been evaluated using the climate atlases of Gorshkov (1983) and Khrol (1996a). In comparing the reanalysis depictions to the atlases, the evaluation is based on the positioning of the prominent features that are generally located along the perimeter of the basin. Quantitative comparison is more difficult because of the limited number of contours shown in the atlases; however, some area averages of the atlas data are available for 70°–90°N.

The average spatial distributions of forecast $P - E$ from the two reanalyses are shown in Fig. 2. In contrast to lower latitudes, where E has been found to be erroneously greater than P over land surfaces (Stendel and Arpe 1997), the ERA forecast $P - E$ distribution is more plausible over the north polar cap and is qualitatively similar to the synthesized climatologies. The average spatial distribution is dominated by low values of between 10 and 20 cm yr^{-1} over most of the central ice pack region with concentrated regions of larger values in the North Atlantic and the Pacific coast of North America.

A concentrated area of maximum values in the ERA occurs along the southeastern coast of Greenland, with an additional precipitation belt along the west coast. The reanalysis precipitation distributions over Greenland have been reviewed by Bromwich et al. (1998a). Although the interior plateau appears to be too dry—less than 10 cm yr^{-1} versus approximately 24 cm yr^{-1} observed at Summit (e.g., Bolzan and Strobel 1994)—the overall spatial distribution for Greenland is in reasonable agreement with glaciological syntheses, such as that constructed by Ohmura and Reeh (1991).

Maximum values for the ERA average $P - E$ field are also present along the Norwegian coast. A large area of E greater than P extends offshore in the Norwegian and Barents Seas between Scandinavia and Svalbard, in agreement with the Gorshkov atlas (Gorshkov 1983). This results from the large values of E extending north from the Atlantic Ocean. The largest values of $P - E$, greater than 220 cm yr^{-1}, occur along the Gulf of Alaska coast. A comparison of annual cycles for various locations in the Arctic from the ERA shows a general progression from summer minima in the North Atlantic toward early spring minima in the Canadian northern territories and Siberia. This is in qualitative agreement with Gorshkov (1983).

To better understand the $P - E$ distribution in the Norwegian Sea, Fig. 3 shows the average spatial distribution of E from the ERA, which is dominated by larger values in the North Atlantic. The spatial distribution of forecast E over the north polar cap shows the Atlantic sector as the only region where values exceed 30 cm yr^{-1}. ERA values of E exceed 80 cm yr^{-1} in selected locations of the Norwegian Sea. This is actually smaller than values shown by Gorshkov (1983), which have contours of 100 cm yr^{-1} for small regions. The average spatial patterns of the ERA and Gorshkov are

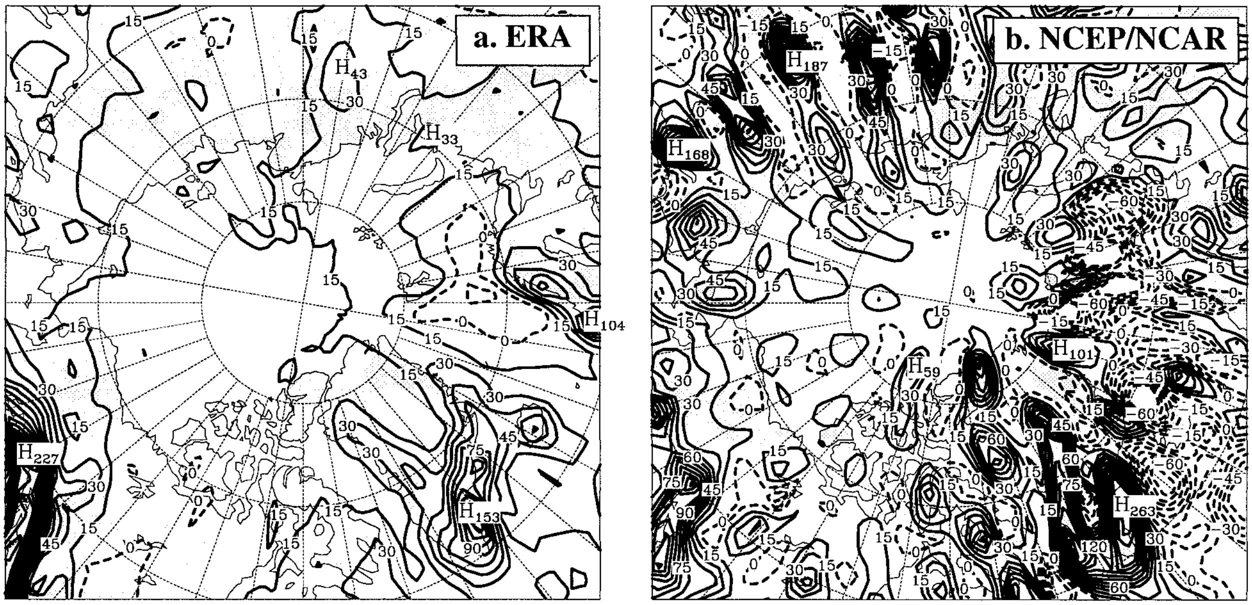

Fig. 2. Spatial distribution of forecast $P - E$ from (a) ERA and (b) NCEP–NCAR, averaged for 1979–93. The contour interval is 15 cm yr^{-1}.

very similar, however, and it is difficult to determine the differences in the average value over large areas.

In contrast to the ERA, the distribution of the NCEP–NCAR $P - E$ field (Fig. 2b) is a significantly busier field, owing to the spurious wave pattern. In addition to P, the forecast E values also contain the spurious wave pattern; however, the wave pattern for the two variables is offset such that large positive values are found in close proximity to locations where E is greater than P. This pattern is particularly evident over Siberia. NCEP has attempted to address the problem via the development of a postprocessing algorithm, but for P only (B. Kistler and M. Iredell 1996, personal communication). The correction identifies the bull's-eyes as spurious moisture sources and removes them in comparison to a diffusion-corrected moisture amount, subject to a temperature threshold. Specifically, the projection of precipitation on an adjusted moisture source value is computed and removed from the precipitation rate. Moisture source is adjusted based on temperature such that it is set to zero when 2-m temperature is above 10°C, used fractionally when 2-m temperature is between below 0°C and 10°C, and the full value used for temperatures below 0°C. The corrected NCEP P has been examined over Greenland by Bromwich et al. (1998a), and the average spatial distribution for the Arctic basin is shown in Fig. 4. It is apparent from examination of the corrected field over Greenland that the problem is with the distribution, rather than the amount of atmospheric moisture. The corrected precipitation field, although an improvement in the spatial distribution, is overly dry in comparison to the original field and the ERA north of 70°N. This leads to a contrast between northern and southern Greenland that is greater than found in synthesized climatologies. Additionally, over central Greenland the temperature threshold of the correction does not allow for the complete removal of the spurious maximum that extends over the relatively colder regions of the high plateau. For other locations in the Arctic basin, the corrected spatial distribution is found to be an obvious improvement over the original

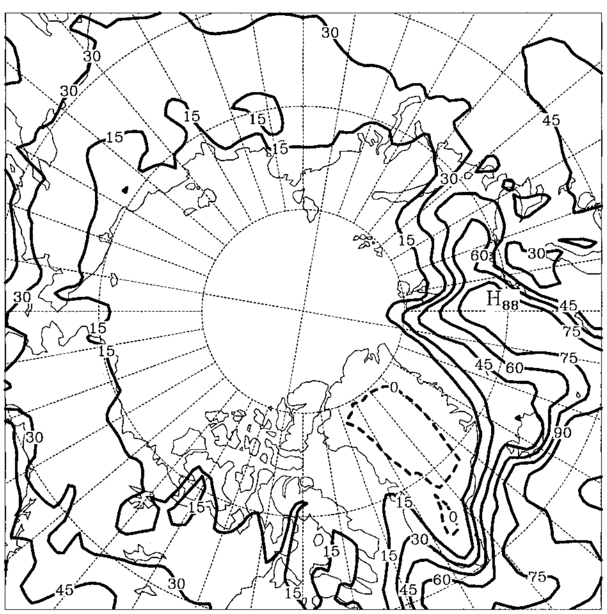

Fig. 3. Spatial distribution of annually averaged forecast E from the ERA over the Arctic basin for 1979–93. The contour interval is 15 cm yr^{-1}.

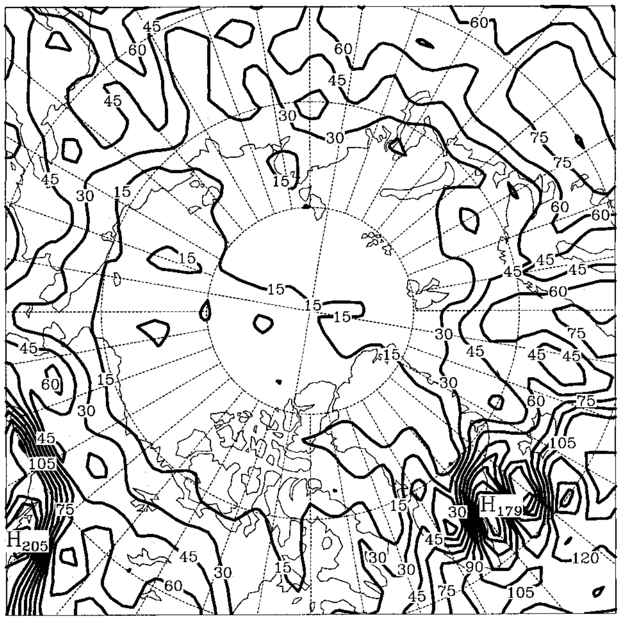

FIG. 4. Spatial distribution of corrected P from NCEP postprocessing of reanalysis forecasts over the Arctic basin, averaged for the period 1979–93. The contour interval is 15 cm yr^{-1}.

field, although significant differences exist in comparison to the ERA and the climatological atlases. Values are generally smaller for the corrected NCEP over the central Arctic basin than for the ERA; average values of less than 15 cm yr^{-1} occur over a large area of the central Arctic for the corrected NCEP, while ERA values of P are greater than 20 cm yr^{-1} over most of the Arctic Ocean. Both the Gorshkov and Khrol atlases indicate an intermediate solution, with the 15 cm yr^{-1} contour confined to within the Canadian basin. Significantly, the corrected NCEP field shows smaller precipitation values for Norway, in contrast to the ERA and both atlases, which show values greater than 100 cm yr^{-1} along the western Scandinavian coast. There is also an additional bull's-eye minimum for the corrected NCEP data in the Denmark Strait that does not appear to be supported by observations. In general, the spatial distribution of the corrected NCEP P contains discrepancies with the climatological atlases in the North Atlantic.

Reanalysis values of P have been compared with gauge data for the central Arctic basin. The Union of Soviet Socialist Republics (USSR) operated drifting ice stations in the Arctic for the period 1950–91 (Radionov et al. 1997). These camps obtained daily gauge estimates of P. Figure 5a shows the trajectories of seven stations

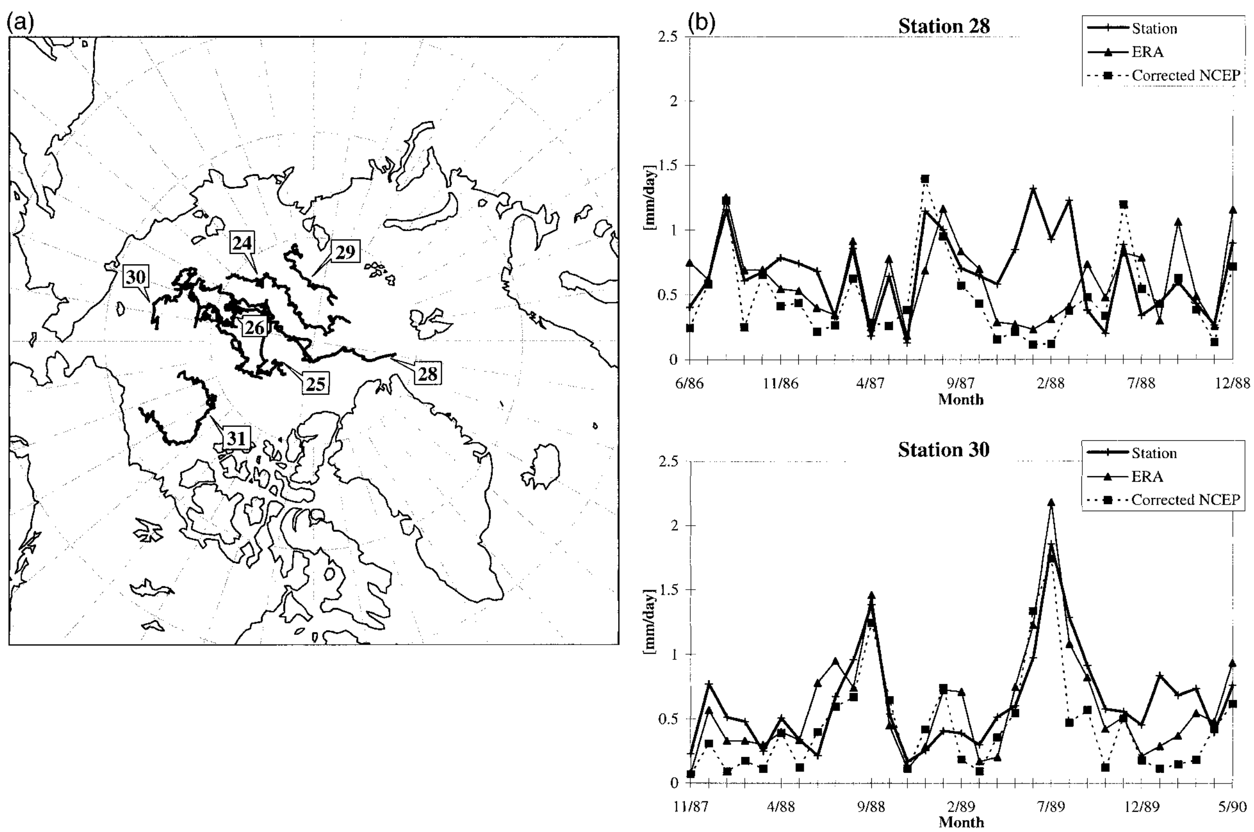

FIG. 5. (a) Trajectories of seven USSR drifting ice stations in the central Arctic for the period 1979–91. (b) Time series of monthly averaged gauge values for stations NP-28 and NP-30 in comparison to corresponding forecast values of the ERA and NCEP corrected P, in mm day^{-1}.

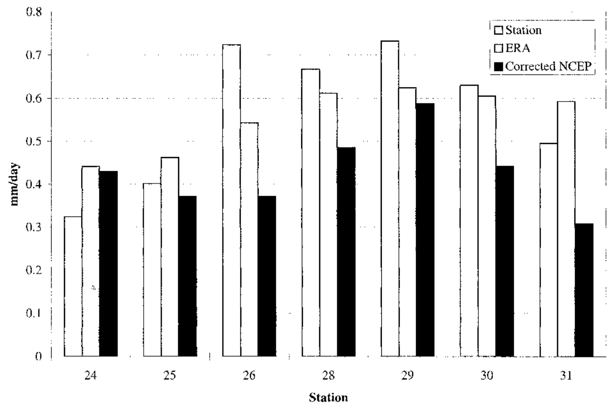

FIG. 6. Average values of P from gauge measurements, forecast ERA, and corrected NCEP data for the duration of each USSR drifting station, in mm day^{-1}. The duration of each station is: NP-24, 22 months; NP-25, 34 months; NP-26, 18 months; NP-28, 31 months; NP-29, 11 months; NP-30, 32 months; NP-31, 27 months.

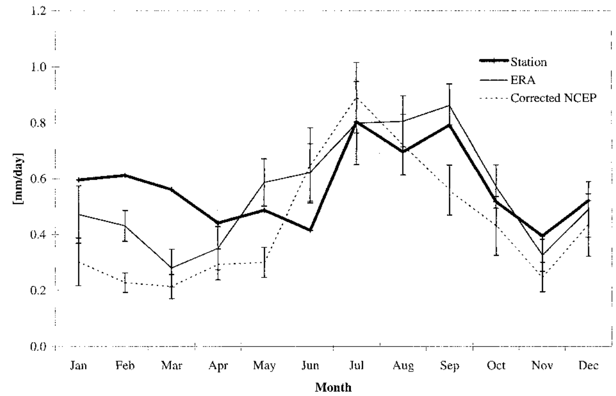

FIG. 7. Monthly mean P from USSR gauge data for the period 1979–91 and discrete, corresponding values from ERA and NCEP corrected forecasts, in mm day^{-1}. Shaded area indicates the standard error of gauge data monthly means. Error bars indicate the standard error of monthly means for the reanalyses.

that were in operation during the 1979–93 time period. Six of the seven stations are clustered over the central ice pack north of 80°N, while station 31 traveled around the Beaufort gyre. A comparison of ERA and corrected NCEP forecast P from the nearest grid point with the camp data encounters numerous difficulties including location questions, the representativeness of one gauge for a grid box, and the reliability of gauge measurements in polar regions. In fact, the day-to-day observations are a poor match with both reanalyses. When the observations and corresponding reanalysis data are composited into monthly averages, however, there is better agreement on the average quantity. Figure 5b shows the time series of monthly values for stations NP-28 and NP-30, which operated in the central Arctic from June 1986 until December 1988, and November 1987 until May 1990, respectively. Station 28 shows significant discrepancies over a limited number of months, while station 30 shows two summertime maxima that are adequately captured by both reanalyses' data. The former is more representative of the station comparisons. Of the seven stations examined, time series of monthly averages from two (stations 30 and 31) show reasonable correlation with the reanalysis data ($r^2 > 0.55$) while the other stations show mediocre to poor agreement ($r^2 < 0.2$ for both datasets). The typical station duration is 25 months. The two stations with reasonable agreement contain the more recent data and were active after November 1987. This suggests that the trend toward better agreement between gauge measurements and forecast P may reflect the increase in the number of meteorological observations available for the central Arctic, particularly from the International Arctic Buoy Program (Thorndike and Colony 1980). In Fig. 6, the average values of the reanalysis forecast P and gauge data are shown for each station. The corrected NCEP values are less than the ERA and typically less than the gauge values by a substantial margin. For example, corrected NCEP values for station NP-26, which operated from July 1983 until December 1984, are 49% smaller than the gauge estimate, while the ERA is 25% smaller than the average observed value. In Fig. 7, the monthly mean precipitation values from gauge data and discrete, corresponding values from reanalysis data have been averaged to produce an annual cycle for the central Arctic. Data for station 31, located south of 80°N, and months with fewer than 10 daily observations have been discounted in producing the figure. The corrected NCEP precipitation average (0.44 mm day^{-1}) was found to be 23% lower than the annual estimate for gauge data of 0.57 mm day^{-1}. Most of this difference occurs in the late winter and spring. The corrected NCEP average annual time series is more peaked than the gauge data, with maximum values in July. The ERA data show better agreement on the shape of the annual cycle, although discrepancies with gauge estimates are also present for February and March. The annual average for the ERA, 0.55 mm day^{-1}, is also much closer to the gauge data.

For the north polar cap region bounded by 70°N, the average forecast P values for 1979–93 are 24.7 cm yr^{-1} for the ERA, 28.6 cm yr^{-1} for the NCEP–NCAR reanalysis, and 13.1 cm yr^{-1} for the corrected NCEP data. For comparison, the improved climatology using gauge measurements from Soviet drifting stations and gauge-corrected station data for Eurasia and Canada by Serreze and Hurst (2000) has an average value of 27.9 cm yr^{-1}, while a value of 29.3 cm yr^{-1} has been computed from the maps of the Khrol atlas (J. E. Walsh 1998, personal communication). These values, as well as the comparison for central Arctic gauge data, show favorable agreement with the ERA forecast P, while corrected NCEP P values are low. Observational estimates for E are more difficult to obtain; however, Khrol (1996b) has tabulated zonal averages of the surface latent heat flux, which may be directly compared with reanalysis forecast data. Averaged for 70°–90°N the Khrol estimate is 6.5 W m^{-2}.

For the period 1979–93, the average reanalysis forecast values are 9.4 W m^{-2} for the ERA and 13.8 W m^{-2} for the NCEP–NCAR reanalysis. It is difficult to assess these comparisons as the atlas estimates are likely to have been determined from observations taken over a long period of time and are not concurrent with the reanalysis data. The relatively close agreement between forecast P and climatology, however, suggests that reanalyses values of E are too high. This is despite comparable spatial patterns of E for the ERA forecasts and the Gorshkov atlas. Differences between reanalyses forecast P and the Khrol climatology are within 16% and 3% for the ERA and NCEP–NCAR reanalyses, respectively, while the differences in the average surface latent heat flux are 45% and 110%.

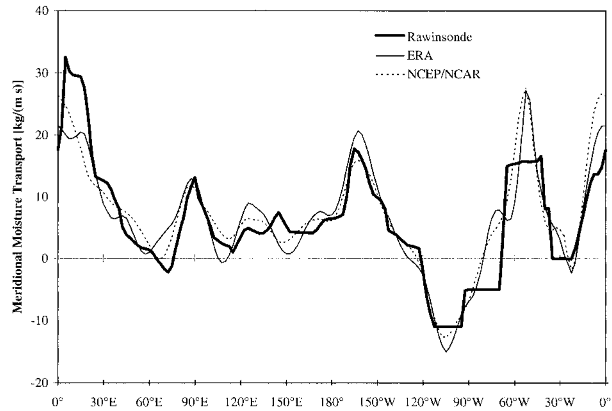

FIG. 8. Annually averaged meridional moisture transport distribution across 70°N from rawinsonde data synthesized after Serreze et al. (1995a), ERA, and NCEP–NCAR reanalysis data, for 1979–93 in kg m^{-1} s^{-1}.

4. Computed $P - E$ from analyzed winds, moisture, and surface pressure

Previous study of moisture convergence by Serreze et al. (1995a,b) employed the HARA data for computing the atmospheric moisture budget over the north polar cap. The HARA data have been compiled primarily from archives at NCAR and the National Climatic Data Center. The spatial distribution of rawinsonde stations that were used to compute the meridional flux across 70°N is shown in Fig. 1. Figure 1 is slightly misleading because of the large variability in the station network. For a typical month, approximately 30 to 40 of the 56 stations shown are actually available.

For the computed $P - E$ [(Eq.) 1], the first term of interest is precipitable water (W). Average values of precipitable water for the north polar cap from the reanalyses have been evaluated using a blended dataset from the National Aeronautics and Space Administration Water Vapor Project (NVAP; Randel et al. 1996). For the Arctic basin, NVAP is primarily composed of retrievals from the Television and Infrared Operational Satellite Operational Vertical Sounder as well as rawinsonde data using quality control described by Ross and Elliot (1996). The NVAP dataset is available for the years 1988–92. Precipitable water averaged for 70°–90°N exhibits peak values in July, with a prolonged period of steady but low winter values from November until March. Precipitable water retrievals from TOVS are subject to some uncertainty over sea ice (e.g., Francis 1994); thus the evaluation may be considered as a comparison of methods rather than a validation of the reanalyses. Annual averages for the period 1988–92 are 6.3 mm for NVAP, 5.8 mm for the ERA, and 6.1 mm for NCEP–NCAR. The differences between the two reanalyses and NVAP are at a minimum in June and July, about 1%–2%. In contrast, the winter months of November to March show larger differences that are reflected in the discrepancies between the annual values. For the five winter months the NVAP average is 3.1 mm compared with the ERA value of 2.5 mm, and NCEP–NCAR, 2.7 mm. The average ERA value is smaller for all months with the exception of July. This is consistent with the known surface temperature cold bias (Kållberg 1997). In general, the agreement of the average values of the NVAP and the reanalyses appears to be consistent with the expected uncertainties.

For computations of the Arctic moisture budget using the HARA data, Serreze et al. (1995a,b) first determined the distribution of the meridional transport along 70°N for each month, and then averaged these data to produce a multiyear mean annual cycle. The computations were performed in this order for the purpose of retrieving the seasonal to interannual variability. The studies by Serreze et al. (1995a,b) were for the years 1974–91, while the ERA is available for the period 1979–93. To eliminate this time difference, the rawinsonde data have been averaged for the time period concurrent with the reanalysis data. A comparison of the average meridional distribution along 70°N for 1979–93 is shown in Fig. 8. The average meridional transport from the rawinsonde synthesis is 6.0 kg m^{-1} s^{-1}, yielding a moisture convergence value for the north polar cap of 17.0 cm yr^{-1}. This compares with the rawinsonde estimate of 16.3 cm yr^{-1} for the period 1973–91 given by Serreze et al. (1995a). It is seen that there are several preferred corridors of poleward moisture transport on the annual average near 20°E, 160°W, and 50°W, with average equatorward moisture flux present only over the western Canadian archipelago near 110°W. Both of the reanalysis datasets produce a larger average moisture transport. The average ERA meridional transport across 70°N is 6.6 kg m^{-1} s^{-1}; for the NCEP–NCAR reanalysis, the value is 7.0 kg m^{-1} s^{-1}. These correspond to convergence values of 18.4 and 19.8 cm yr^{-1}, respectively. The disagreement between the rawinsonde synthesis and reanalysis data has been investigated in detail below; however, it may be immediately seen in Fig. 8 that the rawinsonde data encounter some resolution difficulty over the Baffin Island/Greenland region between 30° and 120°W.

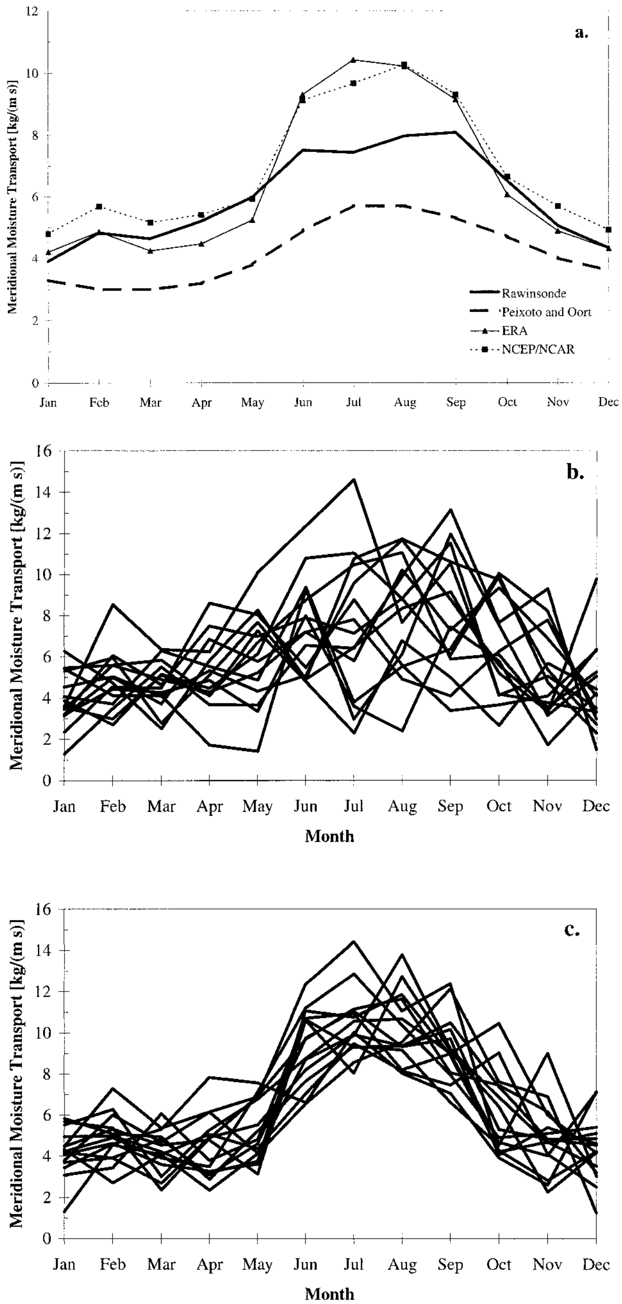

FIG. 9. (a) Average annual cycle of vertically integrated meridional moisture transport across 70°N from reanalyses and synthesized from rawinsonde data, for the period 1979–93 in kg m^{-1} s^{-1}. (b) As in (a) but for individual years from rawinsonde syntheses. (c) As in (a) but for individual years from the ERA.

Figure 9a shows a comparison of the average annual cycle for meridional moisture transport across 70°N. Surprisingly large differences are found between the rawinsonde synthesis and the reanalysis data for summer months, particularly July and August. The reanalysis data then have a fundamentally different depiction of the annual cycle, with a smoothed, unimodal curve and maximum poleward transport in July or August, while the rawinsonde data suggest that the seasonal cycle is much weaker. These differences are even more striking when the year-to-year variability in the annual cycle is examined, as shown in Figs. 9b,c. In general, the curve shown by the ERA is highly reproducible; the annual cycle for each individual year shows very similar characteristics. Not shown, the NCEP–NCAR reanalysis annual cycles have very similar characteristics to those shown for the ERA in Fig. 9c. In contrast, the annual cycles for individual years produced from the rawinsonde data, shown in Fig. 9b, have significant year-to-year variability, particularly in the summer months.

For comparison, Fig. 9a also shows the annual cycle depicted by Peixoto and Oort (1992; see their Fig. 12.21) obtained from rawinsonde data for the period 1963–73. The estimate by Peixoto and Oort (1992) of 12.2 cm yr^{-1} is substantially smaller than that given by Serreze et al. (1995a). Serreze et al. (1995a) attribute the discrepancy to either differences in the stations used or interannual variability. Two issues that arise from the comparison with Peixoto and Oort (1992) are the magnitude and shape of the annual cycle. While the Peixoto and Oort data contain smaller values in comparison to both the rawinsonde synthesis and the reanalysis data, there is agreement between the shape of the annual cycles for Peixoto and Oort (1992) and the reanalysis data. The comparison is intriguing; however, it is difficult to assess the differences between the two rawinsonde syntheses without a detailed inspection of the raw station data. For the present, differences between the Serreze et al. (1995a) and reanalysis data are evaluated.

These differences with the previous study may first be narrowed in time and then in space. For the 15-yr period, time series comparisons have been constructed of the year-to-year average transport across 70°N for each month. Both reanalyses and the rawinsonde syntheses agree very closely on the average value and on the year-to-year variability during the winter. It is only during the summer months of June to August when the significant discrepancies occur. Figure 10 shows a comparison of the average meridional moisture transport distribution along 70°N for July. As with the annual values shown in Fig. 8, it is clear that the limited number of station locations reduces the resolution of the rawinsonde data over the eastern Canadian archipelago and Greenland. This creates a ''stair-stepped'' pattern in the rawinsonde data for the approximate region 30°–120°W. If the reanalysis depictions of the meridional transport along 70°N shown in Fig. 10 are accurate, then it is not surprising that the differences with the rawinsonde data are largest in the summer months, when the meridional transport gradients along 70°N are substantial and tend to expose the limited data resolution in these areas.

Because of the stair-stepped pattern of the rawinsonde synthesis, difference plots of the curves shown in Fig. 10 are intricate, but are characterized by large differences for three regions: western Siberia (80°–100°E),

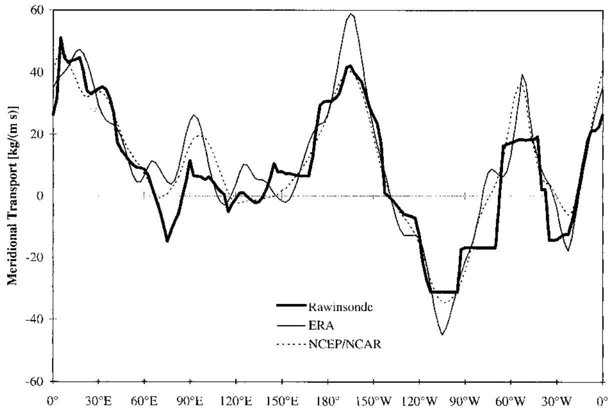

FIG. 10. Comparison of the zonal distribution of the meridional moisture flux across 70°N for July from reanalyses and synthesized from rawinsonde data, averaged for the period 1979–93 in kg m^{-1} s^{-1}. Shaded areas indicate the standard error of the mean from monthly rawinsonde synthesis values.

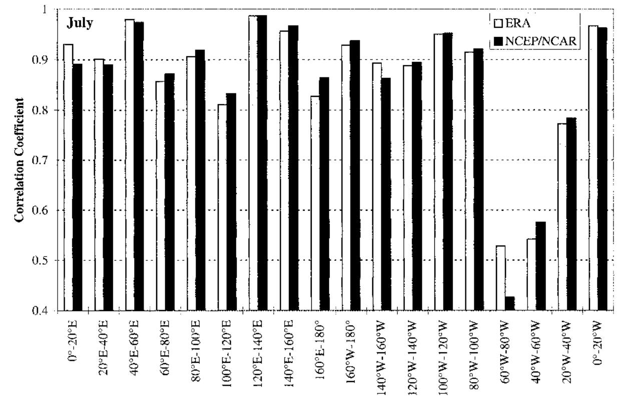

FIG. 11. Correlation coefficients of July mean values for 1979–93 for reanalyses and rawinsonde synthesis values in 20° long intervals.

Chukchi Sea (160°–180°W), and the Davis Strait (60°–80°W). For the Chukchi Sea region, the ERA are significantly different from the rawinsonde synthesis, while the NCEP–NCAR reanalysis is in agreement.

In Fig. 11, correlation coefficients are computed for time series of July mean values from the rawinsonde synthesis and the reanalyses. Figure 11 indicates that the interannual variability is not captured for the Greenland/Baffin Island region. The correlation between reanalysis and rawinsonde syntheses are particularly low for the region 60°–80°W for both the ERA ($r^2 = 0.28$) and the NCEP–NCAR ($r^2 = 0.18$). This contrasts with more reasonable values for western Siberia (ERA and NCEP–NCAR: $r^2 > 0.81$) and the Chukchi Sea (ERA: $r^2 = 0.86$, NCEP/NCAR: $r^2 = 0.88$). Thus the discrepancies for the western Siberian and Chukchi Sea regions are essentially biases, with the interannual variability adequately produced.

In the vicinity of Greenland, the discrepancies between rawinsonde syntheses and reanalyses are due to deficiencies in the rawinsonde network. For a subregion of the Davis Strait bounded by 47.5° and 55°W and containing the largest discrepancies, the disagreements can be directly related to difficulties in the rawinsonde network. As shown in Fig. 12, large differences occur between rawinsonde and reanalysis data only when data for the Egedesminde rawinsonde station along the western Greenland coast (69°N, 53°W) are unavailable, as occurred in July 1981 and July 1988. By ‘‘unavailable,’’ this means that there were less than 20 soundings in the archive for the month that passed the quality control criteria established by Serreze et al. (1992), and these data were discarded. Under these circumstances the rawinsonde synthesis relies on estimates from Thule and southern Baffin Island stations to resolve the transport over the Davis Strait. The average flux difference between the reanalyses and the rawinsonde synthesis for these two years is about five times larger than for the other years. It is also known that some difficulties arose with the rawinsonde data from the Canadian archipelago region used in the rawinsonde synthesis. These stations did not always contain near-surface data.

Similar problems in the rawinsonde network distribution are found for the western Siberian region defined by 67.5°–100°E. Shown in Fig. 13, up to nine stations contribute to the synthesized meridional transport estimates from this region; however, the array of available stations varies considerably from year to year. In the examples shown in Fig. 13, the ERA depicts the moisture transport core in a location where the rawinsonde stations are not reporting (Fig. 13a) and in a location that is between all stations (Fig. 13b). Meridional transport patterns for the NCEP–NCAR reanalysis, not shown, are similar.

These comparisons demonstrate that the differences between reanalysis data and the rawinsonde synthesis occur in the presence of changes in the rawinsonde network. There are no observations that are independent of both methods, however, and it is therefore a more

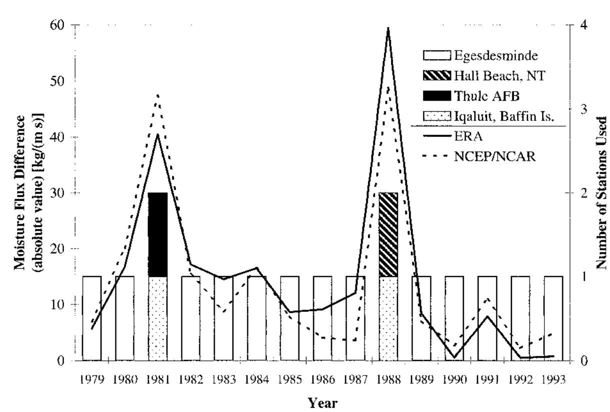

FIG. 12. Time series of the difference in July meridional moisture transport across 70°N for the Davis Strait region (47.5°–55°W) of reanalyses minus the rawinsonde synthesis, in kg m^{-1} s^{-1}. Columns indicate the rawinsonde stations used in the synthesis.

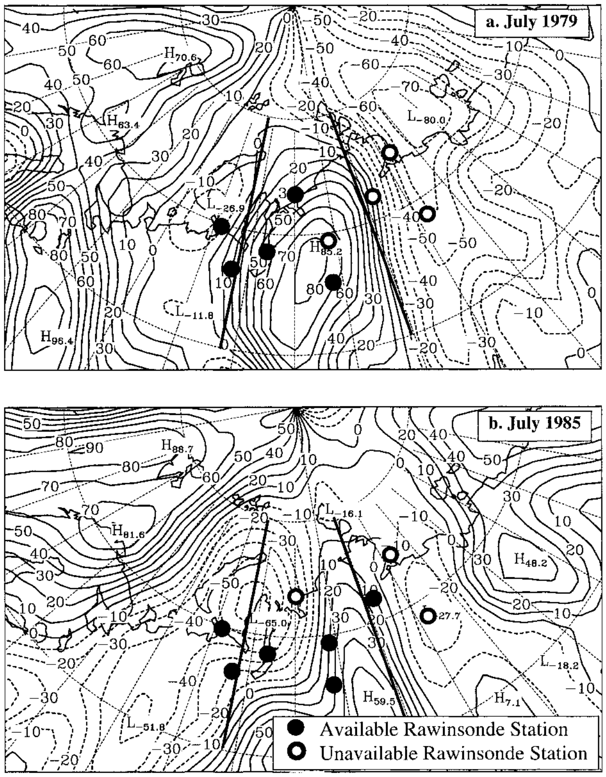

FIG. 13. (a) Contour plot of Jul 1979 ERA meridional moisture transport from over northern Eurasia from the ERA and locations of rawinsonde stations used in computing moisture transport across 70°N between 67.5° and 100°E. The contour interval is 10 kg m^{-1} s^{-1}. (b) As in (a) but for July 1985.

difficult task to indicate that the reanalysis depiction is more realistic. It is apparent, however, that the limitations of the rawinsonde network are highlighted during the summer months because of the larger flux magnitudes and spatial gradients. Reanalysis data also incorporate the rawinsonde data and thus may be thought of as a more elaborate synthesis of these data than the method employed by Serreze et al. Because reanalyses also include other factors including additional surface observations, satellite data, topographic forcing, and the downstream advection of observations via the NWP model, it may be readily understood why the reanalysis data may be more able to overcome missing observations and produce a more realistic depiction. The differences shown in Figs. 9b and 9c are compelling. Given the available evidence, it is concluded that the reanalysis depiction is generally more realistic.

The resolution of differences between the two reanalyses for the Chukchi Sea region appears to be a more difficult task. Although marine rawinsonde data are available for this region, the variability in location and time of the data does not allow for easy determination. Precipitable water values of the two reanalyses are in reasonable agreement, indicating the winds as the primary cause of the discrepancy.

The spatial depictions of the vector-averaged ERA and NCEP–NCAR moisture transports for 1979–93, shown in Fig. 14, reveal a mostly zonal pattern for the interior Arctic basin, with the circulation centered near 90°N. Over most land areas the transport is also approximately zonal, with southerly transport occurring over the Bering Strait and western Alaska, as well as the North Atlantic–Norwegian Sea region. A signature of the Icelandic low is found southeast of Greenland. The interannual variability in the transport field is very large. The annually averaged central Arctic circulation migrates considerably from one year to the next. A year of interest is 1982, when the center of circulation was located near 85°N and 20°E. Averaged for this year, the atmospheric moisture transport through the Fram Strait was from the north, an unusual climatic anomaly. Some differences exist for the central Arctic basin, with the NCEP–NCAR reanalysis depicting moisture transports with a larger meridional component, particularly north of Svalbard. Overall, however, the moisture transport patterns of the two reanalyses are very similar. Although there is general agreement between the reanalyses on the flux patterns, there are significant differences in the convergence fields, shown in Fig. 15. At T21 resolution, both reanalyses capture major features along the southeast coast of Greenland and the Gulf of Alaska; however, the positioning is not great. For example, in both datasets the southeast Greenland maximum is erroneously centered over the Denmark Strait, while values over the interior plateau are negative. Difficulties also exist in both reanalyses over the Mackenzie River in western Canada, where $P - E$ is less than zero over land for the annual average. These inadequacies are reminiscent of the discussion given by Rasmusson and Mo (1996), in which terrain-related biases were noted in the computed $P - E$ of the NCEP operational analyses as compared to the forecast fields at lower latitudes. The significant difference between the two datasets is found in the North Atlantic, with the 30 cm yr^{-1} contour in the NCEP–NCAR reanalysis extending from the North Atlantic through the Fram Strait and over the North Pole. ERA values, in contrast, are generally smaller over the central Arctic basin.

5. Comparison of the two methods

Table 1 compares estimates of computed $P - E$, as well as the forecast values, to previous studies for the north polar cap bounded by 70°N. The original NCEP–NCAR forecast P is used for consistency with the available forecast E. The reanalysis moisture transport for the near-surface level was used in this study but was not considered by Genthon (1998). Both the ERA and the NCEP–NCAR reanalysis are not in hydrologic balance. Computed $P - E$ results are 38% and 73% larger than the forecast data for the ERA and NCEP–NCAR, respectively. This imbalance is summarized in Figs. 16 and 17. In Fig. 16, the annually averaged zonal profiles

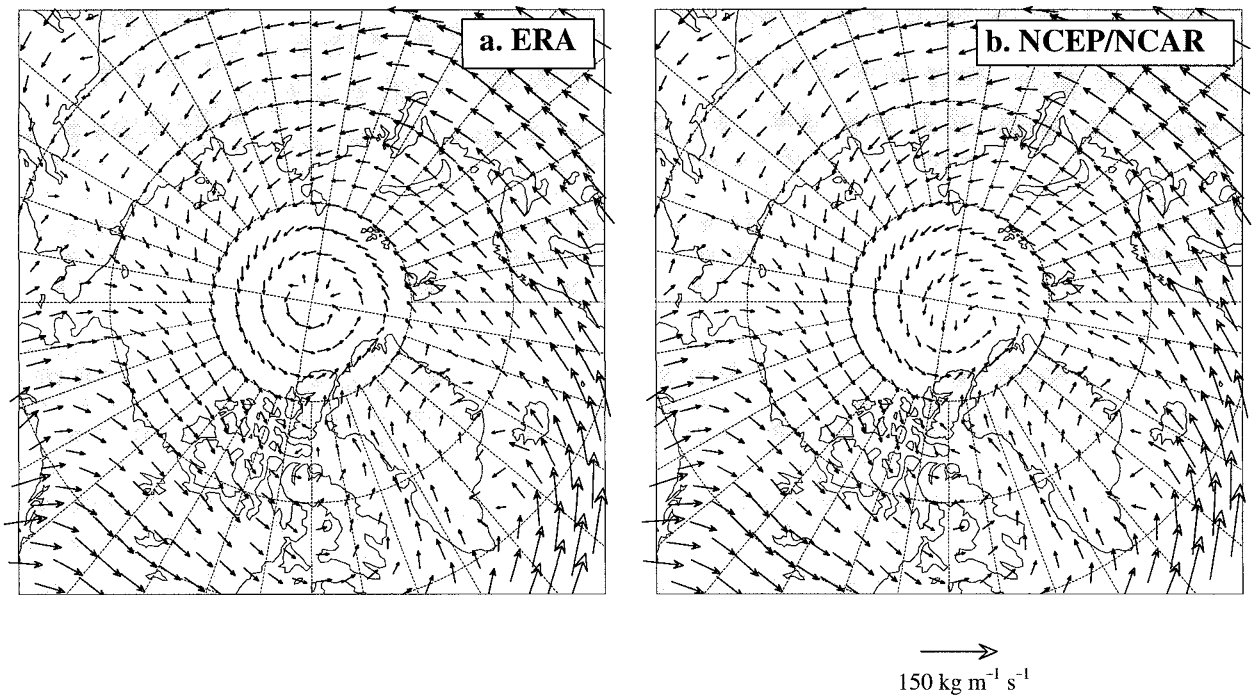

FIG. 14. Average spatial pattern of the vector-averaged total moisture transport from (a) ERA and (b) NCEP–NCAR reanalysis, for the years 1979–93.

show that the computed $P - E$ values are higher than the forecasts for both datasets at nearly all latitudes poleward of 50°N. From 75° to 85°N, the imbalances of the two datasets are similar at about 5 cm yr^{-1}. Equatorward of 75°N, the imbalance in both datasets becomes larger; however, this is particularly true of the NCEP–NCAR reanalysis. The NCEP–NCAR imbalance is consistent with Trenberth and Guillemot (1996b, 1998), who show the discrepancies to be larger in the presence of the higher-magnitude $P - E$ values along the Pacific coast of North America, the southeast coast of Geenland, and the Greenland–Norwegian Seas re-

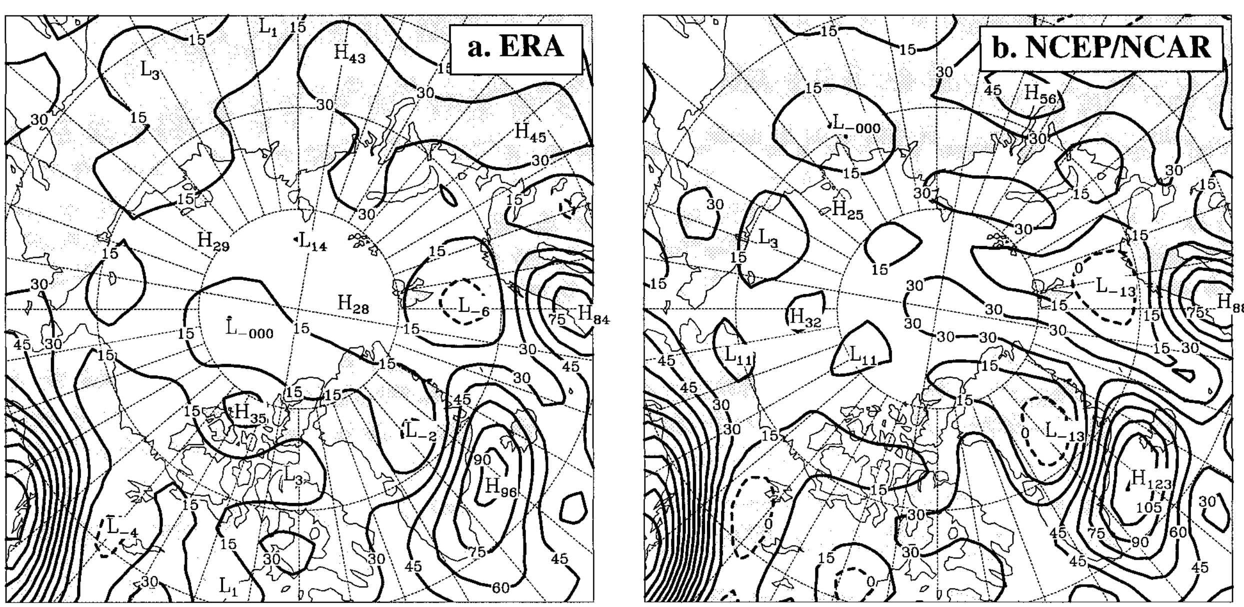

FIG. 15. Average annual spatial distribution of atmospheric moisture transport convergence computed from (a) ERA and (b) NCEP–NCAR reanalysis for 1979–93 at T-21 resolution. The contour interval is 15 cm yr^{-1}.

TABLE 1. Comparison of estimates of $P - E$ for the north polar cap bounded by 70°N. Asterisk denotes preferred values, as explained in the text.

	Dataset time period	$P - E$, 70°–90°N (cm yr^{-1})
Based on surface data		
Sellers (1965)	multiyear	5.0
Baumgartner and Reichel (1975)	multiyear	6.1
Korzoun et al. (1977a,b)	multiyear	20.4*
Based on rawinsonde data (computed $P - E$)		
Peixoto and Oort (1983)	1963–73	12.2
Overland and Turet (1994)	1965–90	21.4*
Serreze et al. (1995a,b)	1974–91	16.3*
Based on numerical analyses (computed $P - E$)		
Masuda (1990), ECMWF FGGE analyses	1979	15.5*
Genthon (1998), ERA	1979–93	20.7*
This study, ERA	1979–93	18.2*
This study, NCEP–NCAR	1979–93	19.4*
Based on NWP forecasts (forecast $P - E$)		
Genthon (1998), ERA forecasts	1979–93	12.9
This study, ERA forecasts	1979–93	13.2
This study, NCEP–NCAR forecasts (original data)	1979–93	11.2

gion. In Fig. 17, the annual cycles for $P - E$ for both methods and datasets are shown for the polar cap. The hydrologic balance of both reanalysis datasets does not remain constant with the annual cycle. The largest discrepancies occur in the summer months, which is consistent with deficiencies in forecast E suggested earlier in comparison to values given by Khrol (1996b). In both datasets, a maximum in forecast E occurs in May, and this is reflected by the very large imbalance for this month. For the ERA, the imbalance ranges from 7% of computed $P - E$ in January to 64% in May, while the NCEP–NCAR imbalance ranges from 15% to 91% for the same months.

In Table 1, a general progression may be seen in previous studies from smaller values to contemporary estimates of between 15 and 21 cm yr^{-1}. The surface data studies are based on separate estimates of P and E. For the Korzoun et al. (1977a,b) study, which is in better agreement with rawinsonde data, the estimate of P is approximately 73% larger than either Sellers (1965) or Baumgartner and Reichel (1975). The Korzoun et al. value is also identical to that determined by Walsh's analysis of the Khrol atlas (J. E. Walsh 1998, personal communication). Thus preferred values may be selected from Table 1 by eliminating the earlier surface-based studies, the lower values of Peixoto and Oort (1983) described earlier, and the NWP forecast values. Using the remaining preferred estimates denoted by the asterisk, an average of 18.9 cm yr^{-1} is found with a standard deviation of 2.3 cm yr^{-1} among estimates. This is in reasonable agreement with the model result of the NCAR Community Climate Model version 3 of 18.1 cm yr^{-1} (Briegleb and Bromwich 1998). In comparison, estimates based on NWP forecasts have an average of

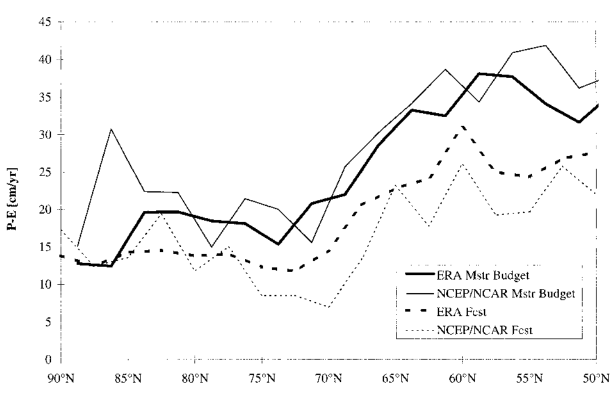

FIG. 16. Zonal comparison of average annual $P - E$ computed from ERA and NCEP–NCAR reanalysis moisture transports and forecast fields for 1979–93 in cm yr^{-1}.

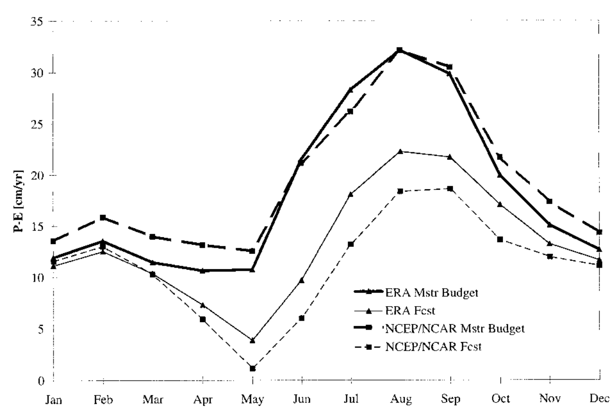

FIG. 17. Comparison of average monthly $P - E$ over 70°–90°N computed from reanalysis moisture transports and forecast fields for 1979–93 in cm yr^{-1}.

12.4 ± 1.0 cm yr^{-1}. This appraisal of Table 1 strongly implies that the estimates based on NWP forecasts are low by at least 3.2 cm yr^{-1} or approximately 19%.

6. Summary and discussion

There are significant differences between $P - E$ of each reanalysis dataset. At the top of the list is the spurious wave pattern seen in the raw NCEP–NCAR forecast precipitation fields. The NCEP–NCAR corrected forecast P field is qualitatively similar to that of the ERA; however, it is much drier. Comparison of reanalysis computed $P - E$ from analyzed winds, moisture, and surface pressure reveals general agreement between the two datasets. For instance, computed $P - E$ from both models captures the major features along the southeast coast of Greenland and in the Gulf of Alaska. In addition, both identify a region of negative computed $P - E$ between the Barents and Norwegian Seas. At high northern latitudes, the most notable exception in agreement of computed $P - E$ is the NCEP–NCAR portrayal of large values (30 cm yr^{-1}) northeast of Greenland extending northward through the Fram Strait and over the North Pole. This feature is not present in the computed ERA $P - E$ field.

Comparison between forecast and computed values of $P - E$ provides information regarding drift of the numerical weather prediction model used in the data assimilation process; the imbalance represents the transition from the observationally constrained initial conditions to a climate preferred by the model. In this case, both models tend toward a drier average surface balance. As with the Antarctic (Bromwich et al. 1998b), observational estimates of E in the Arctic are extremely scarce. There is little information concerning the data for the estimates by Khrol (1996b), which serve as the primary source of climatological evaporation data. However, the evidence compiled here strongly supports the estimates of $P - E$ computed via the atmospheric moisture budget as being much more realistic than the forecast values, with the major source of the hydrologic imbalance being the forecast E fields.

Analysis of forecast $P - E$ from reanalyses and observational data reveal some discrepancies among these data sources. As alluded to above, comparison with surface latent heat flux values from Khrol (1996b) as well as the comparison in Table 1 indicate that forecast E for both reanalyses is too large by a significant amount. Comparisons with climate atlases and in situ gauge measurements indicate reasonable agreement with forecast P from the ERA. There are some discrepancies in temporal comparisons with gauge data, as shown in Fig. 5b. Forecast P from the NCEP–NCAR reanalysis contains substantial discrepancies associated with the diffusion parameterization in the NWP model. A corrected NCEP forecast P variable is an obvious improvement; however, discrepancies remain with climatology, particularly for the North Atlantic.

For the computed atmospheric moisture budget $P - E$, the discrepancy in the shape of the annual cycle with previous rawinsonde analysis is related to inadequacies in the rawinsonde network. As mentioned earlier, Serreze et al. (1995a,b) first computed the monthly transport distribution along 70°N for the purpose of retrieving the monthly and interannual variability. When the order of computations is reversed—that is, when long-term flux climatologies are computed for each station, and then a distribution along 70°N is produced—the agreement with the reanalysis data is not improved. Several other sensitivities have been considered in the rawinsonde synthesis, including the radius of influence for each station, and the spatial resolution of the transport distribution. Sensitivity to these parameters is large but does not alter the overall conclusions.

It remains to be seen whether the rawinsonde estimate can be rectified with a different method or enhanced using additional observations. It is apparent from the compiled HARA data that several stations contain records that abruptly end and then begin again. Data for missing months and/or additional stations may be available from alternative sources. The difficulties of the rawinsonde synthesis leave the reanalyses as the only source for depicting interannual variability. From the reanalyses, $P - E$ estimates obtained from the moisture budget approach are preferred to the forecast values. In addition, moisture flux from ERA appears to give the best results overall when compared with Russian climatologies. Part II of this paper will address the issue of interannual variability of the Arctic hydrologic cycle using the reanalyses. While the reanalysis datasets represent a significant advance toward understanding the atmospheric hydrologic cycle over the Arctic basin, additional efforts are required to improve these data.

Since completion of this manuscript, the NCEP-Department of Energy Atmosphere Model Intercomparison Project-2 reanalysis became available through NCEP. This improves upon the NCEP–NCAR reanalysis by fixing errors and improving some of the physical parameterizations, and will span 1979–97. In particular, the spectral noise problem in the NCEP–NCAR forecast P and E described here has been corrected. The resulting $P - E$ distribution (not shown) is a smoothed version of that given in Fig. 2a for EKA, but has lower values.

Acknowledgments. ECMWF data and the NCEP–NCAR reanalyses were obtained from NCAR. This research was sponsored by the National Aeronautics and Space Administration under Grant NAG5-6001 to the second author and by the National Science Foundation under Grant OPP-9614297 to the third author.

REFERENCES

Adams, J. C., and P. N. Swarztrauber, 1997: Spherepack 2.0: A model development facility. NCAR Tech. Note NCAR/TN-436-STR, 58 pp. [Available from the National Center for Atmospheric Research, P.O. Box 3000, Boulder, CO 80307.]

Baumgartner, A., and E. Reichel, 1975: *The World Water Balance.* Elsevier, 179 pp.

Bolzan, J. F., and M. Strobel, 1994: Accumulation-rate variations around Summit, Greenland. *J. Glaciol.,* **40,** 56–66.

Briegleb, B. P., and D. H. Bromwich, 1998: Polar climate simulation of the NCAR CCM3. *J. Climate,* **11,** 1270–1286.

Broecker, W. S., 1997: Thermohaline circulation, the Achilles heel of our climate system: Will man-made CO_2 upset the current balance? *Science,* **278,** 1582–1588.

Bromwich, D. H., R. I. Cullather, Q.-S. Chen, and B. M. Csathó, 1998a: Evaluation of recent precipitation studies for Greenland Ice Sheet. *J. Geophys. Res.,* **103,** 26 007–26 024.

——, ——, and M. L Van Woert, 1998b: Antarctic precipitation and its contribution to the global sea level budget. *Ann. Glaciol.,* **27,** 220–226.

Cullather, R. I., D. H. Bromwich, and M. L. Van Woert, 1998: Spatial and temporal variability of Antarctic precipitation from atmospheric methods. *J. Climate,* **11,** 334–367.

Francis, J. A., 1994: Improvements to TOVS retrievals over sea ice and applications to estimating Arctic energy fluxes. *J. Geophys. Res.,* **99,** 10 395–10 408.

Genthon, C., 1998: Energy and moisture flux across 70°N and S from ECMWF Re-Analyses. *Proc. First WCRP Int. Conf. on Reanalyses,* WCRP-104 (WMO/TD-No. 876), Silver Spring, MD, WMO, 371–374.

Gibson, J. K., P. Kållberg, S. Uppala, A. Hernandez, A. Nomura, and E. Serrano, 1997: ERA description. ECMWF Re-Analysis Project Report Series 1, 72 pp. [Available from ECMWF, Shinfield Park, Reading, RG2 9AX, United Kingdom.]

Gorshkov, S. G., Ed., 1983: *Arctic Ocean. World Ocean Atlas,* Vol. 3, Pergamon Press, 189 pp.

Kållberg, P., 1997: Aspects of the re-analysed climate. ECMWF Re-Analysis Project Report Series 2, 89 pp. [Available from ECMWF, Shinfield Park, Reading, RG2 9AX, United Kingdom.]

Kalnay, E., and Coauthors, 1996: The NCEP–NCAR 40-year reanalysis project. *Bull. Amer. Meteor. Soc.,* **77,** 437–471.

Key, J., and M. Haefliger, 1992: Arctic sea ice surface temperature retrieval from AVHRR thermal channels. *J. Geophys. Res.,* **97,** 5885–5893.

Khrol, V. P., 1996a: *Atlas of the Water Balance of the Northern Polar Area.* Gidrometeoisdat, 81 pp.

——, 1996b: *Energy Balance of the Northern Polar Sea.* Gidrometeoisdat, 168 pp.

Korzoun, V. I., A. A. Sokolov, K. P. Voskresensky, G. P. Kalinin, A. A. Konoplyantsev, E. S. Korotkevich, and M. I. Lvovich, 1977a: *World Water Balance and Water Resources of the Earth.* UNESCO Press, 663 pp.

——, ——, ——, ——, ——, ——, and ——, 1977b: *Atlas of World Water Balance.* UNESCO Press, 36 pp. + 65 maps.

Masuda, K., 1990: Atmospheric heat and water budgets of polar regions: Analysis of FGGE data. *Proc. NIPR Symp. Polar Meteor. Glaciol.,* **3,** 79–88.

Mysak, L. A., D. K. Manak, and R. F. Marsden, 1990: Sea-ice anomalies observed in the Greenland and Labrador seas during 1901–1984 and their relation to an interdecadal Arctic climate cycle. *Climate Dyn.,* **5,** 111–133.

Newell, R. E., and Y. Zhu, 1994: Tropospheric rivers: A one-year record and a possible application to ice core data. *Geophys. Res. Lett.,* **21,** 113–116.

Ohmura, A., and N. Reeh, 1991: New precipitation and accumulation maps for Greenland. *J. Glaciol.,* **37,** 140–148.

Overland, J. E., and P. Turet, 1994: Variability of the atmospheric energy flux across 70°N computed from the GFDL data set. *The Polar Oceans and Their Role in Shaping the Global Environment. The Nansen Centennial Volume, Geophys. Monogr.,* No. 85, Amer. Geophys. Union, 313–325.

Peixoto, J. P., and A. H. Oort, 1983: The atmospheric branch of the hydological cycle and climate. *Variations in the Global Water Budget,* A. Street-Perrott, M. Beran, and R. Ratcliffe, Eds., D. Reidel, 5–65.

——, and ——, 1992: *Physics of Climate.* American Institute of Physics, 520 pp.

Randall, D., and Coauthors, 1998: Status of and outlook for large-scale modeling of atmosphere–ice–ocean interactions in the Arctic. *Bull. Amer. Meteor. Soc.,* **79,** 197–219.

Randel, D. L., T. H. von der Haar, M. A. Ringerud, G. L. Stephens, T. J. Greenwald, and C. L. Combs, 1996: A new global water vapor dataset. *Bull. Amer. Meteor. Soc.,* **77,** 1233–1246.

Rasmusson, E. M., and K. C. Mo, 1996: Large-scale atmospheric moisture cycling as evaluated from NMC global analysis and forecast products. *J. Climate,* **9,** 3276–3297.

Ross, R. J., and W. P. Elliott, 1996: Tropospheric water vapor climatology and trends over North America: 1973–93. *J. Climate,* **9,** 3561–3574.

Rossow, W. B., C. L. Brest, and L. C. Gardner, 1989: Global, seasonal surface variations from satellite radiance measurements. *J. Climate,* **2,** 214–247.

Sellers, W. D., 1965: *Physical Climatology.* University of Chicago Press, 272 pp.

Serreze, M. C., and J. A. Maslanik, 1997: Arctic precipitation as represented in the NCEP/NCAR reanalysis. *Ann. Glaciol.,* **25,** 429–433.

——, and C. M. Hurst, 2000. Representation of mean Arctic precipitation from NCEP–NCAR and ERA reanalyses. *J. Climate,* **13,** 182–201.

——, J. D. Kahl, and S. Shiotani, 1992: The Historical Arctic Rawinsonde Archive documentation manual. Special Rep. 2, National Snow and Ice Data Center, University of Colorado, 26 pp. [Available from NSIDC, Campus Box 449, University of Colorado, Boulder, CO 80309-0449.]

——, R. G. Barry, and J. E. Walsh, 1995a: Atmospheric water vapor characteristics at 70°N. *J. Climate,* **8,** 719–731.

——, M. C. Rehder, R. G. Barry, J. E. Walsh, and D. A. Robinson, 1995b: Variations in aerologically derived Arctic precipitation and snowfall. *Ann. Glaciol.,* **21,** 77–82.

Stendel, M., and K. Arpe, 1997: Evaluation of the hydrologic cycle in reanalyses and observations, ECMWF Re-analysis Project Report Series 6, 62 pp. [Available from ECMWF, Shinfield Park, Reading, RG2 9AX, United Kingdom.]

Thorndike, A. S., and R. Colony, 1980: Arctic Ocean Buoy Program. Polar Science Center Data Report, 19 January 1979 to 31 December 1979, 131 pp. [Available from Polar Science Center, Applied Physics Laboratory, University of Washington, 1013 NE 40th Street, Seattle, WA 98105-6698.]

Trenberth, K. E., 1995: Atmospheric circulation climate changes. *Climatic Change,* **31,** 427–453.

——, and C. J. Guillemot, 1996a: Physical processes involved in the 1988 drought and 1993 floods in North America. *J. Climate,* **9,** 1288–1298.

——, and ——, 1996b: Evaluation of the atmospheric moisture budget and hydrologic cycle in the NCEP reanalysis. NCAR Tech. Note NCAR/TN-430+STR, 300 pp. [Available from National Center for Atmospheric Research, P.O. Box 3000, Boulder, CO 80307.]

——, and ——, 1998: Evaluation of the atmospheric moisture budget and hydrologic cycle in the NCEP/NCAR reanalysis. *Climate Dyn.,* **14,** 213–231.

Woo, M.-K., R. Heron, P. Marsh, and P. Steer, 1983: Comparison of weather station snowfall with winter snow accumulation in high Arctic basins. *Atmos.–Ocean,* **32,** 733–755.